COMPARATIVE ANALYSIS ON MONOLITHIC DENOX CATALYSTS

CLAUDIO FERONE[1], RAFFAELE CIOFFI[1], STEFANO CIMINO[2], LUCIANA LISI[2],
SIMONE MALVEZZI[3] & GIOVANNI PERILLO[4]
[1]Dipartimento di Ingegneria, Università di Napoli "Parthenope", Italy
[2]Consiglio Nazionale delle Ricerche, Istituto di Ricerche sulla Combustione, Italy
[3]A2A, Corso di Porta Vittoria 4, Italy
[4]Wessex Institute of Technology, UK

ABSTRACT

Catalysts based on the Vanadia-Titania system are widely used for the abatement of pollutants, particularly nitrogen oxides (NO_x), in the exhaust gases of industrial plants. Their mechanism of operation is based on the catalytic reduction reaction of nitrogen oxides with ammonia (SCR). In this paper, two commercial catalysts based on the V-W-Ti system of very similar nominal composition were compared. The two samples were analyzed in the fresh state and after a period of operation in a waste-gas plant of a waste-to-energy plant. The materials were first characterized from the chemical-structural point of view through instrumental techniques such as X-ray fluorescence (XRF), X-ray diffractometry (XRD), IR spectroscopy (FT-IR), SEM scanning electron microscopy observations with analysis EDS, measurement of pore size and specific surface area through nitrogen adsorption/desorption and BET technique. Subsequently, the catalytic properties of the new and used catalysts in the NH3-SCR reaction were evaluated. The results of the analyzes showed that the samples are both made of a titanium matrix in the form of anatase, reinforced with glass fibers, used as a support for the active phases based on V and W. The percentages of vanadium are practically the same for both systems, while the tungsten percentage is very different. The specific surface also has very similar values for the two fresh catalysts. The tests of catalytic activity, on the other hand, have given very different results, particularly for one of the two catalysts, the performance decays much faster than the other. The kinetic measurements show that the decay is not due to a specific surface decrease, due to the presence of precipitates, but to a difference in initial activity between the two catalysts, linked to the different tungsten content.
Keywords: Vanadia-Titania, SCR, DeNOx.

1 INTRODUCTION

Catalysts used for the treatment of the pollutants contained in the exhaust gases are generally produced by adding catalytically active materials to a monolithic structure. Diluted contaminants can be removed in the presence of a high gas–solid contact surface, combined with acceptable pressure drops.

This study is focused on the application of $DeNO_x$ catalysts based on Vanadia-Titania systems for the selective catalytic reduction reaction (V-SCR):

$$4NO + 4NH_3 + O_2 \rightarrow 4N_2 + 6H_2O. \tag{1}$$
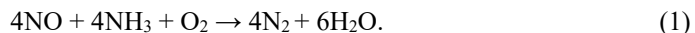
The supported V-based catalysts have a long history and have been extensively studied in the literature [1]. Regarding the SCR reaction, generally the catalyst acts by reacting the adsorbed ammonia on Lewis and Brønsted acid sites with weakly bound or gaseous NO. The commercial SCR catalysts consist of a mixture of Anatase (TiO_2), tungsten, vanadium and small percentages of aluminosilicates; they are found on the market in monolithic form or as plates, although usually the most used form, for this particular process, is the monolithic honeycomb, obtained industrially through the extrusion process. These catalysts

are in great commercial demand due to their multiple characteristics, such as activity in a wide temperature range, high stability and low oxidative activity against SO_2. In fact, sulfur dioxide can be oxidized to SO_3 according to the reaction:

$$SO_2 + \tfrac{1}{2}\, O_2 \rightarrow SO_3. \qquad (2)$$

The vanadium pentoxide has a high activity not only in the reduction of nitrogen oxides but also in the previous oxidation reaction [2]. This reaction is undesirable because the sulfuric anhydride produced reacts with ammonia and water to form sulfate $((NH_4)_2SO_4)$ and ammonium bisulphate (NH_4HSO_4) [3]:

$$2NH_3 + SO_3 + H_2O \rightarrow (NH_4)_2SO_4, \qquad (3)$$

$$NH_3 + SO_3 + H_2O \rightarrow (NH_4)HSO_4. \qquad (4)$$

These sulfates tend to settle and accumulate on the catalyst, causing a poor performance of NO_x removal performance. For this reason, the percentage of V in the catalyst cannot be too high and must be carefully optimized. To reduce oxidative activity in respect of SO_2, WO_3 is also added, which in turn is also an active catalyst in the SCR reaction [4].

Two samples of commercial $DeNO_x$ catalysts were analyzed and compared, similar in type, but different as producers. The same samples were then analyzed after a period of operation in a waste-to-exhaust system of a waste-to-energy plant, in order to evaluate any deterioration in aging. The 4 samples will be called Sample A, Sample B, Sample A18, Sample B30, where 30 and 18 represent the time of use of the catalyst sample in the plant, expressed in kh.

The virgin and aged samples were first characterized from the chemical-mineralogical and microstructural point of view, then the catalytic activity in the SCR reaction was evaluated.

2 MATERIALS AND METHODS

2.1 Materials

The analyzed catalyst samples are parallelepiped shaped extrusions with dimensions of 15 cm × 15 cm × 105 cm and are characterized by the presence of internal channels with a square section on the 3.5 mm side (Fig. 1).

Figure 1: Catalyst samples used in the experimentation.

2.1.1 Samples A and B

In consideration of the fact that the samples were not exposed to any process, in each case only one portion of catalyst of height equal to about 3 cm was taken. The sections studied were taken from the end of the sample and appear yellowish in color. The amount to be used for the chemical-physical analyzes provided has been taken from the central part of each sample portion.

2.1.2 Samples A18 and B30

Two portions of catalyst with a height of about 3 cm were taken. The first was taken from the end of the gas inlet sample, which appears reddish in color, different from the yellowish color shown by the other parallelepiped base, very similar to what could be observed for the second portion taken from the center of the parallelepiped. From the center of each sample portion the amounts of catalyst to be used for the intended analyzes were taken.

2.2 Methods

2.2.1 Chemical analysis

The chemical analysis of the catalysts was performed by X-ray fluorescence (XRF) using a Bruker M4 Tornado instrument.

2.2.2 Mineralogical analysis

The mineralogical analysis of the catalysts was performed by X-ray diffractometry (XRD), using a Rigaku Miniflex 600 instrument with the following acquisition parameters:

Radiation $Cu_{k\alpha}\lambda = 1.54060$ nm; Range 2θ $3 – 90°$; step $0.02°$; time per step 0.1 s.

2.2.3 Fourier transform infrared spectroscopy (FT-IR) analysis

The FT-IR absorption spectra were recorded in the 4000–400 cm^{-1} range using a Nicolet system, Nexus model, equipped with a DTGS KBr detector. A spectral resolution of 2 cm^{-1} was chosen. Each test sample (2.0 mg) was mixed with 200 mg of KBr in an agate mortar and then pressed into tablets with a diameter of 13 mm. The spectrum of each sample represents an average of 32 scans.

2.2.4 Microstructural analysis

The microstructural analysis of the samples was performed by scanning electron microscopy (SEM) with coupled energy dispersion microsonde (EDS). A Phenomworld instrument from Phenomworld was used, equipped with an energy dispersion microprobe for chemical analysis.

2.2.5 Porosimetric analysis

The porosimetric analysis was performed through N_2-adsorption measurements at 77 K with a Quantachrome Autosorb 1-C apparatus.

2.2.6 Catalytic activity test in the NH3-SCR reaction

The catalytic reactor consists of a quartz tube with an internal diameter of 10 mm. The fixed catalyst bed (0.125g, h ≈ 2mm) is supported by a layer of quartz wool and is made using particles with controlled granulometry in the 125–200 μm range (obtained by grinding and sieving samples taken from the monolithic elements at honeycomb) without further dilution. The catalytic reactor is positioned inside a cylindrical electric oven with

PID control of the three independent heating zones. The reaction temperature of the catalytic bed was measured using a type K thermocouple positioned inside the reactor, about 1 cm above the catalyst bed. The catalytic tests were conducted in the temperature range 90–550°C. The gaseous feed rate was set at 25 L/h (at 25°C and 1 bar), which corresponds to a GHSV space velocity of 160,000 h^{-1}. The very high value of the selected GHSV and the small dimensions of the catalyst particles have allowed to extend the operating temperature range in which the catalyst is working in a purely kinetic manner, without the measured conversion and selectivity data being influenced by the emergence of phenomena of resistance to the transport of matter. The concentrations of the main gaseous species involved in the SCR process were measured continuously with two series analyzers, respectively for NH_3 (GEIT) for NO, NO_2, N_2O (Emerson X-Stream) with independent measurement crews based on IR and UV detectors (for N_2O). The ammonia analyzer has a laser technology source that guarantees minimal interference with the other species present in the gas stream (in particular water). Between the two analyzers a Sycapent trap is interposed for the removal of the unreacted ammonia and of the water before the NO_x measurement.

The production of N_2 (desired reaction product) was calculated from the atomic nitrogen balance, in the absence of formation of other compounds containing nitrogen. The conversions of NO and of NH_3 and the selectivity of the process at N_2 were calculated from the concentrations of the gaseous species through the following formulas:

$$NO_x \text{ conversion} (\%) = \frac{[NO_x]_{in} - [NO_x]_{out}}{[NO_x]_{in}} \times 100,$$

$$NH_3 \text{conversion} (\%) = \frac{[NH_3]_{in} - [NH_3]_{out}}{[NH_3]_{in}} \times 100,$$

$$N_2 \text{ selectivity} (\%) = \frac{[N_2]_{out}}{[N_2]_{out} + [N_2O]_{out}} \times 100.$$

3 RESULTS

3.1 Chemical analysis

The chemical composition of Samples A and B is shown in Table 1.

It can be observed that the percentage of V_2O_5, active catalytic component, is practically the same in the two samples, while the percentage of WO_3 in the Sample B is almost double compared to the Sample A.

3.2 Mineralogical analysis

The analysis of the X-ray diffraction spectrum of Samples A and B (Fig. 2) allows the precise identification of a single crystalline phase, the anatase (TiO_2, JCPDS), since all the main diffraction peaks present in the diffractogram are attributable to this phase. The

Table 1: Chemical composition of Samples A and B expressed as a percentage by weight.

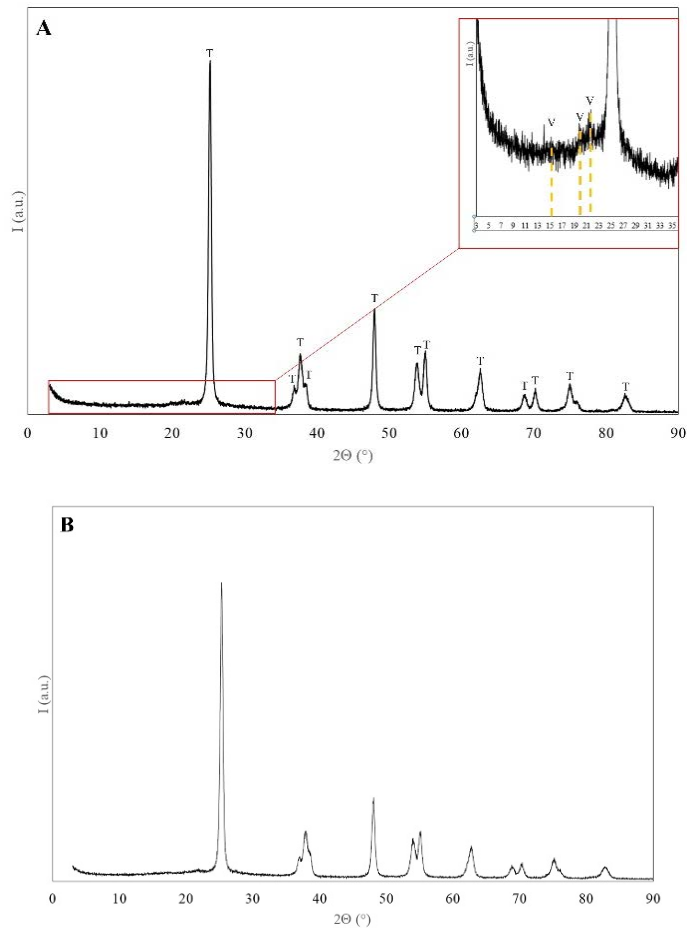|	TiO$_2$	WO$_3$	V$_2$O$_5$	SiO$_2$	Al$_2$O$_3$	CaO	Fe$_2$O$_3$	NiO	MnO$_2$
A	85.53	6.36	3.51	2.01	1.10	1.14	0.30	0.03	0.01
B	78.42	11.42	3.36	3.69	1.13	1.81	0.16	-	0.02

Figure 2: Diffraction spectra of Samples A and B.

diffractograms of Samples C and D are not shown as they are completely analogous to those of the virgin samples. In the zoom window of Fig. 2(a) we can see extremely low intensity diffraction peaks which are not attributable to anatase and which are compatible with V_2O_5 composition phases (phase name, JCPDS card).

A precise attribution is not possible, given the extremely low intensity of the same peaks. The absence of well-defined diffraction peaks attributable to phases V and W indicates that the same phases are well distributed on the surface of the support [5]. Similar considerations can also be made for the diffractometric analyzes of Samples B, A18 and B30.

3.3 Analysis in infrared spectroscopy

Analysis by FTIR spectroscopy confirms the presence, both in Sample A and in Sample B (Fig. 3), of titanium dioxide in the form of anatase and vanadium pentoxide and tungsten trioxide [6].
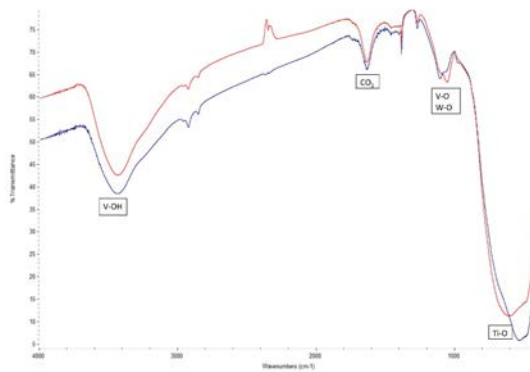
Figure 3: FT-IR spectrum of Samples A (red curve) and B (blue curve).

No changes in the curves of the aged samples are observed (not shown).

3.4 Scanning electron microscopy analysis

The following are the results of the microscopic observations performed on the two Samples A and B. The parts examined were taken from the walls of the catalyst channels (Fig. 4). On each fragment, observations were made at different points on the surface (Figs 5(a)–(c) and 6(a)–(c)) and on the fracture section (Figs 5(d)–(f) and 6(d)–(f)) in order to analyze the structure of the wall itself.

The observations in electron microscopy allow to identify the presence of reinforcing fibers in both samples, clearly evident from the observations of the fracture surfaces (Figs 5(e), 5(f), 6(e) and 6(f)).

The chemical analyzes carried out with the EDS microprobe confirm the presence of Ti, W and V in the matrix and make it possible to determine that the reinforcing fibers consist of silica glass containing Al, Ca and B.

These observations confirm the fact that the catalysts are constituted by a network of glass fibers, coated with the TiO_2 anatase phase, containing the elements W and V [7].
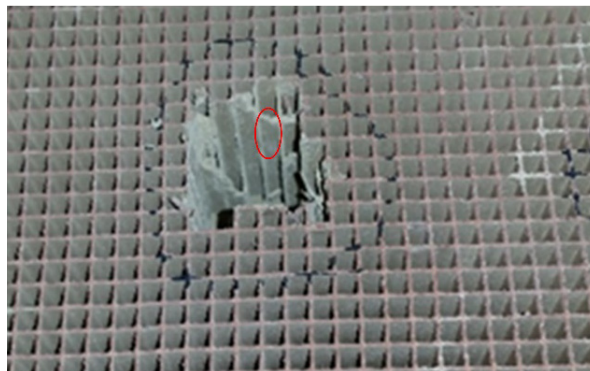

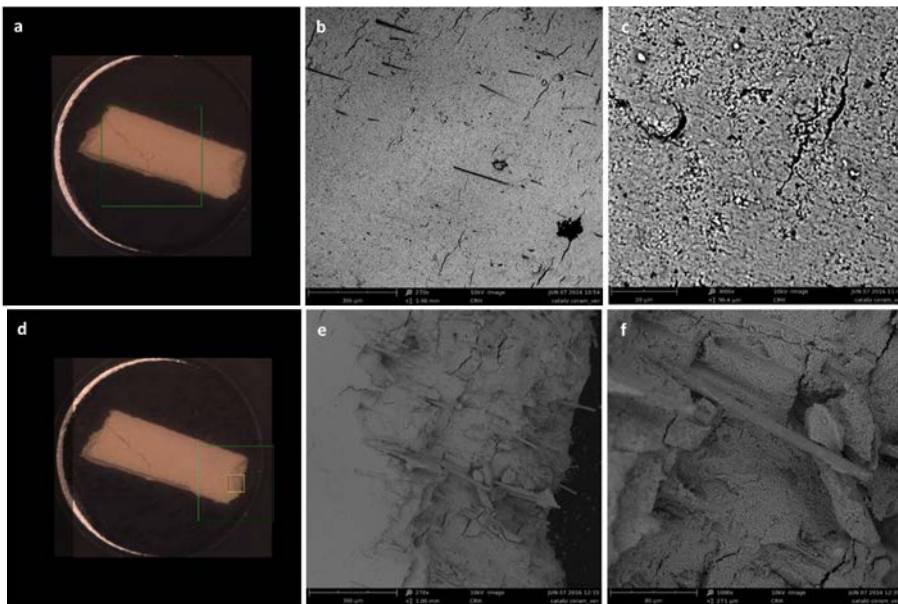Figure 4: Indication of the sampling point and the area observed at the SEM.

Figure 5:   Sample A. Optical microscopy of the surface and fracture section (a) and (d) observed in electron microscopy at different magnifications (b), (c), (e) and (f).
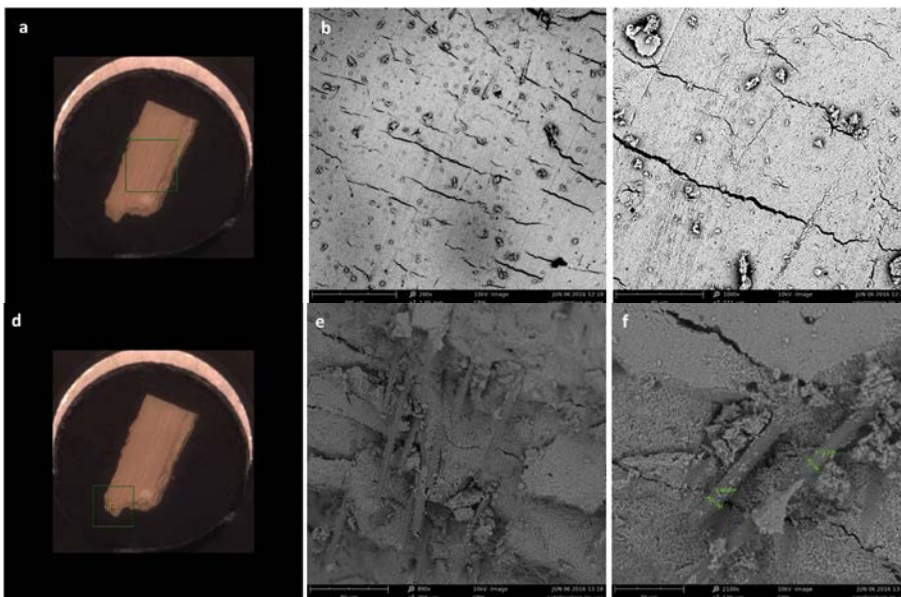

Figure 6:   Sample B. Optical microscopy images of the surface and of the fracture section (a) and (d) observed in electron microscopy at different magnifications (b), (c), (e) and (f).

3.5 Porosimetric analysis

Fig. 7 shows the adsorption isotherms of N_2 at 77 K on virgin catalysts A and B. The isotherms for both materials show an analogous trend throughout the partial pressure range and indicate the typical behavior of mesoporous materials with a modest microporosity content.

The two virgin catalysts are characterized by initial values of the specific surface area very similar to each other (difference around 7%) with a slight advantage for the B system compared to A (Table 2).

The porosimetric distribution was calculated with the BJH method starting from the points on the desorption branch of the respective isotherms (Fig. 7(b)). Catalyst A has a single-mode distribution of mesopores with sizes between 80 and 300 Å and centered at about 125 Å. Catalyst B has a bimodal distribution of pores with a prevalence of mesopores of characteristic sizes ranging from 50–300 Å centered at about 100 Å, in addition to which a small amount of smaller pores with a characteristic size of around 25 Å is observed. The analysis of the low pressure branch of the isotherms (P/P0 < 0.01) conducted with the SF method suggests for the two catalysts the presence of some micropores with a characteristic size around 8 Å.

The differences between the two catalysts are accentuated after the aging in reaction (Table 2), with the catalyst B which is decidedly more stable and able to maintain about 92% of the starting area after 30,000 hours of operation. On the contrary, the system A aged for 18,000 h undergoes a more evident reduction of surface area, maintaining about 76% of the initial value.
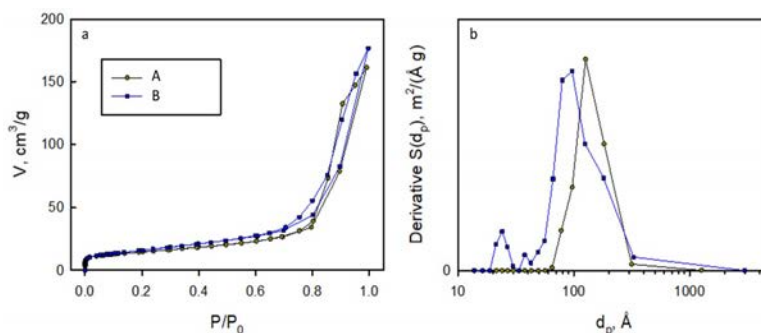

Figure 7: (a) Isotherms of adsorption of N_2 to 77 K; and (b) Porosimetric distribution obtained with BJH method on the desorption branch of the isotherm for Samples A and B.

Table 2: Comparison of the measurements of specific surface area (BET method) and porosity obtained by testing adsorption of N_2 to 77 K on Samples A and B.

Sample	Degas	Weight loss %	BET s.a. m^2/g
A	240°C, 2h	3.5	53.8
B	240°C, 2h	3.3	58.0
A18	240°C, 2h	3.4	42.0
B30	240°C, 2h	3.8	53.6

3.6 Catalytic activity test in the NH$_3$-SCR reaction

Fig. 8 shows the conversion curves of NO and of NH$_3$ measured as a function of the reaction temperature with the virgin catalysts A and B, and with the same after aging in reaction. Under the experimental conditions selected, the fresh commercial catalysts are capable of activating the SCR reaction of NO with NH$_3$ starting from temperatures above 100°C. In all cases we observe a monotonic increasing trend in the conversion of ammonia with the temperature up to 100%. On the contrary, the conversion of NO increases progressively with the temperature up to about 300°C, reaching maximum values between 96 and 98.5%, then stabilizing and finally starting to decrease for temperatures above 350°C. As regards the scale of catalytic activity, it is noted that system B guarantees NO removal performance constantly higher than the corresponding catalyst A at each temperature level. In other words, the lower specific activity of catalyst A determines the need for a reaction temperature of about 25–30°C higher to obtain the same conversion level obtainable with catalyst B.

All the catalytic systems A and B show a total selectivity to N$_2$ during the SCR reaction of NO with NH$_3$ up to the temperature of about 300°C (Fig. 9). Under these conditions, for each NO converted molecule the consumption of a molecule of NH$_3$ is measured, according to the stoichiometry of the SCR reaction. For temperatures above 300°C, a relatively rapid decrease in selectivity to N$_2$ is observed, which depends on the formation of increasing quantities of N$_2$O between the reaction products. Under these conditions the amount of ammonia consumed becomes progressively greater than the amount of NO converted, following the proceeding of reactions other than SCR.

The trend of the selectivity curve at N$_2$ as a function of temperature is practically coincident on systems A and B virgin and on the B aged 30,000 h, while it is slightly worse in the case of the A18 system which is also characterized by a more marked reduction in activity catalytic (lower conversion of NO at each temperature level).
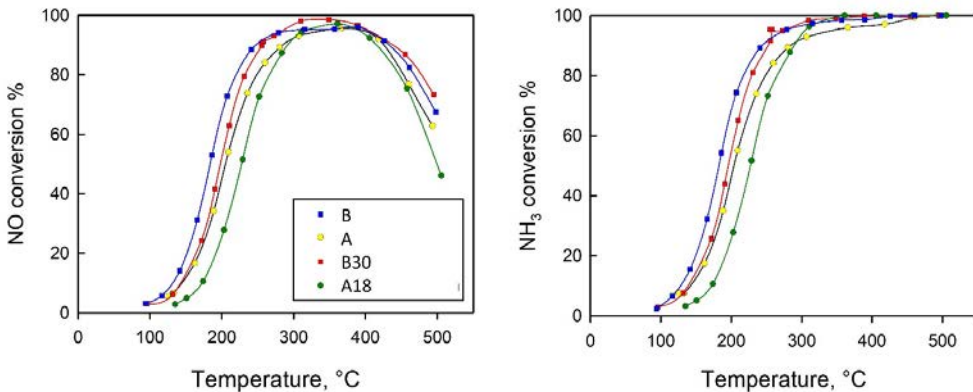

Figure 8:   Trend in the conversion of NO and NH$_3$ as a function of the reaction temperature during the NH$_3$-SCR NO tests performed on commercial catalysts A and B.
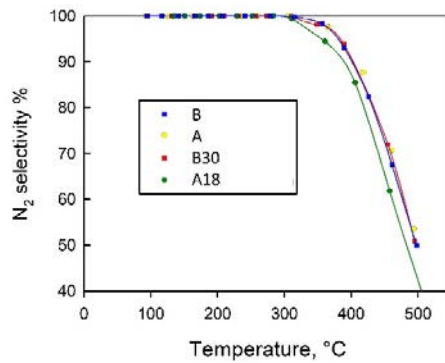
Figure 9: Selectivity to N_2 as a function of the reaction temperature during the NH_3-SCR tests of NO carried out on commercial catalysts A and B.

The experimental results obtained in the reaction tests were used to evaluate the kinetic parameters of the NO SCR reaction on fresh catalysts and after prolonged aging under process conditions. In particular, by modeling the reactor with the isothermal and isobar "plug-flow reactor" hypothesis and considering a first order kinetics in the NO concentration the Arrhenius diagrams of Fig. 10 have been obtained. The linearity of these diagrams in the zone of lower temperature suggests the existence of a purely kinetic regime. The estimates of the kinetic parameters Ea (apparent activation energy) and kw0 (pre-exponential factor) reported in Table 3 can be obtained from the slope and intercept of the regression lines and used for the calculation of the disappearance rate of NO per unit of mass of catalyst (kw) through the formula:

$$k_w = k_w^0 exp\left(-\frac{E_a}{RT}\right)\left[\frac{m^3}{(gs)}\right].$$

For values of ln (kw) higher than -9 there is a progressive reduction in the slope of the Arrhenius plots, connected to the onset of phenomena of resistance to the transport of matter, initially at the intraparticle level.
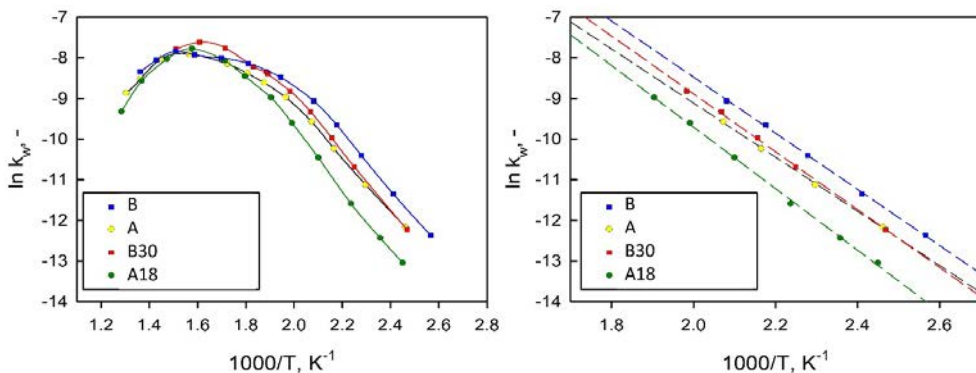

Figure 10: Arrhenius plot for the speed of the NH_3-SCR NO reaction on fresh JM and CERAM commercial catalysts and after prolonged aging in reaction.

Table 3: Estimation of the kinetic parameters Ea and kw0 for the NH_3-SCR reaction of NO and the value of the kinetic constant at 200°C for commercial catalysts A and B.

	E_a	$\ln k_w^0$	k_w (200°C)	Relative activity
	kJ/mol	m^3/(g s)	m^3/(g s)	
A	54.25	3.89	5.02E-05	0.527
B	57.45	5.35	9.53E-05	1.00
A18	62.97	5.44	2.58E-05	0.271
B30	59.24	5.36	5.73E-05	0.601

The estimate of the apparent activation energy of the SCR reaction of NO provides very similar values for the fresh catalysts A and B, around 54–57 kJ/mol, in good agreement with the literature data on catalysts with a similar composition of the active phase [8].

The aging of the catalysts under process conditions determines a reduction in the reaction speed which is accompanied by a slight increase in the apparent activation energy. In detail, the variation of Ea for system B after aging is hardly detectable (from 57–59 kJ/mol); on the contrary, for the catalyst A aged 18,000 h, the calculated value of Ea increases by almost 9 kJ/mol up to 63 kJ/mol. This circumstance suggests that catalyst A has undergone more significant changes in the active phase, not attributable solely to the reduction in surface area, which should not significantly alter the reaction mechanism and activation energy [9]. The data in Table 3 clearly show that the virgin catalyst B is the most active among those tested. Probably, this behavior is linked to the greater content of W compared to Sample A [10]. Normalizing the reaction rates measured at 200°C compared to that obtained on system B, it is observed that the virgin catalyst A has an activity equal to about half. The aging of the system B for 30,000 h results in a reduction of activity of 40% compared to the initial value. For catalyst A, aging in reaction appears to have a greater and above all quicker impact, since the reaction rate at 200°C after only 18,000 h has been reduced to 50% of the initial value. The speed of the SCR reaction on the catalyst B discharged after 30,000 h of reaction is about twice the value measured on Sample A discharged after only 18,000 h in flow.

4 CONCLUSIONS

The two samples of catalyst analyzed, compared to very similar nominal characteristics, provided quite different performances. In fact, the catalyst A after 18,000 operating hours has performances much lower than those of the Sample B after 30,000 hours of operation. This difference in performance cannot be ascribed solely to the decrease in the surface area of the sample, which was determined by the precipitation of solid reaction products but is probably related to the difference in chemical composition. In particular, the cause can be traced back to the lower content of WO_3 in Sample A compared to Sample B.

REFERENCES

[1]   Guerrero-Perez, M.O., Supported, bulk and bulk-supported vanadium oxide catalysts: A short review with an historical perspective. *Catal. Today*, **285**, pp. 226–233, 2017.

[2]   Svachula, J., Alemany, L.J., Ferlazzo, N., Forzatti, P., Tronconi, E. & Bregani, F., Oxidation of SO_2 to SO_3 over honeycomb DeNo$_x$ing catalysts. *Ind. Eng. Chem. Res.*, **32**, p. 826, 1993.

[3]   Xi, Y., Ottinger, N.A. & Liu, Z.G., New insights into sulfur poisoning on a vanadia SCR catalyst under simulated diesel engine operating conditions. *Applied Catalysis B: Environmental*, **160–161**, pp. 1–2, 2014.

[4]   Chen, J.P. & Yang, R.T., Role of WO_3 in mixed V_2O_5-WO_3/TiO_2 catalysts for selective catalytic reduction of nitric oxide with ammonia. *Applied Catalysis A: General*, **80**, p. 135, 1992.

[5]   Zhang, S. & Zhong, Q., Surface characterization studies on the interaction of V_2O_5–WO_3/TiO_2 catalyst for low temperature SCR of NO with NH_3. *Journal of Solid State Chemistry*, **221**, pp. 49–56, 2015.

[6]   Topsoe, N.Y., Characterization of the nature of surface sites vanadia/titania catalysts by FTIR. *Journal of Catalysis*, **128**, p. 449, 1991.

[7]   Coudurier, G. & Védrine, J.C., EUROCAT oxide: A European V_2O_5–WO_3/TiO_2 SCR standard catalyst study: Characterisation by electron microscopies (SEM, HRTEM, EDX) and by atomic force microscopy. *Catalysis Today*, **56**(4), pp. 415–430, 2000.

[8]   Cimino, S., Totarella, G., Tortorelli, M. & Lisi, L., Combined poisoning effect of K+ and its counter-ion (Cl− or NO$_3$−) on MnO_x/TiO_2 catalyst during the low temperature NH_3-SCR of NO. *Chemical Engineering Journal*, **330**, pp. 92–101, 2017.

[9]   Lisi, L., Lasorella, G., Malloggi, S. & Russo, G., Single and combined deactivating effect of alkali metals and HCl on commercial SCR catalysts. *Applied Catalysis B: Environmental*, **50**(4), pp. 251–258, 2004.

[10] He, Y. et al., Influence of catalyst synthesis method on selective catalytic reduction (SCR) of NO by NH_3 with V_2O_5-WO_3TiO_2 catalysts. *Applied Catalysis B: Environmental*, **193**, pp. 141–150, 2016.